Estimation of Shoreline Position and Change using Airborne Topographic Lidar Data

Hilary F. Stockdon†§, Asbury H. Sallenger, Jr.†, Jeffrey H. List‡, and Rob A. Holman§

†U.S. Geological Survey
Center for Coastal Geology
600 4th Street South
St. Petersburg, FL 33701,
  U.S.A.

‡U.S. Geological Survey
Woods Hole Field Center
34 Woods Hole Road
Woods Hole, MA 02543,
  U.S.A.

§College of Oceanic and
  Atmospheric Sciences
Oregon State University
104 Ocean Admin Bldg
Corvallis, OR 97330, U.S.A.

ABSTRACT

STOCKDON, H.F.; SALLENGER, A.H. JR.; LIST, J.H., and HOLMAN, R.A., 2002. Estimation of shoreline position and change using airborne topographic lidar data. *Journal of Coastal Research*, 18(3), 502–513. West Palm Beach (Florida), ISSN 0749-0208.

A method has been developed for estimating shoreline position from airborne scanning laser data. This technique allows rapid estimation of objective, GPS-based shoreline positions over hundreds of kilometers of coast, essential for the assessment of large-scale coastal behavior. Shoreline position, defined as the cross-shore position of a vertical shoreline datum, is found by fitting a function to cross-shore profiles of laser altimetry data located in a vertical range around the datum and then evaluating the function at the specified datum. Error bars on horizontal position are directly calculated as the 95% confidence interval on the mean value based on the Student's t distribution of the errors of the regression. The technique was tested using lidar data collected with NASA's Airborne Topographic Mapper (ATM) in September 1997 on the Outer Banks of North Carolina. Estimated lidar-based shoreline position was compared to shoreline position as measured by a ground-based GPS vehicle survey system. The two methods agreed closely with a root mean square difference of 2.9 m. The mean 95% confidence interval for shoreline position was ± 1.4 m. The technique has been applied to a study of shoreline change on Assateague Island, Maryland/Virginia, where three ATM data sets were used to assess the statistics of large-scale shoreline change caused by a major 'northeaster' winter storm. The accuracy of both the lidar system and the technique described provides measures of shoreline position and change that are ideal for studying storm-scale variability over large spatial scales.

ADDITIONAL INDEX WORDS: *Beach processes, coastal change, remote sensing, storm impact assessment.*

INTRODUCTION

A recent focus in nearshore research has been large-scale coastal behavior (LSCB, THORNTON *et al.*, 2000), changes in nearshore bathymetry and beach topography with spatial scales of order kilometers and temporal scales of order years. It is at these scales that decisions are made in coastal zone management and at these scales that improvement to scientific understanding is needed.

In order to accurately quantify the variability of large-scale coastal changes and to obtain a clearer understanding of the processes driving these changes, detailed measurement of large-scale morphology over regional scales is required. While change occurs over the entire active profile, the horizontal location and movement of the shoreline are two of the most commonly chosen variables of large-scale beach morphology and serve as direct indicators of erosion and accretion. Topographic maps (USGS Quadrangles and NOS Topographic Sheets), rectified aerial photographs, and traditional beach profiles have been the most common source for long-term, large-scale measures of shoreline position (DOLAN *et al.*, 1980). These historical shoreline locations are often compared to present shoreline locations to calculate rates of long-term shoreline change. Because of their long record length, maps

and aerial photographs are invaluable in quantifying long-term shoreline change.

Traditional Shoreline Proxies

Quantification of shoreline location, or the interface between the land and the water, usually involves a number of assumptions. Therefore, all estimates will have error associated with both the technique for measuring shoreline position and the assumptions made regarding the definition of the shoreline. Traditional methods using aerial photographs for shoreline measurement often involved non-stereo photography that has no vertical information. In this case, relationships must be assumed between some identifiable, horizontal feature and its assumed vertical elevation.

For coastal change applications, the location of the high water line (HWL), defined as the landward extent of the last high tide (ANDERS and BYRNES, 1991; CROWELL *et al.*, 1991; DOLAN *et al.*, 1980; STAFFORD, 1971), is commonly used to mark the position of the shoreline. Often the HWL may be difficult to identify or may appear as a gradational zone of change. Here, other physical features, such as the wet/dry line, (CROWELL *et al.*, 1991), vegetation line, drift line, or dune line (MORTON, 1991) are used as a proxy for shoreline location. This leaves the determination of the location of this feature to the judgment of the operator (ANDERS and BYRNES, 1991)

and it may often be confused with the latest swash excursion, a debris line, an erosional scarp, or changes in sediment type or color (CROWELL et al., 1991). Since the relationship of these proxies and an actual tidal datum may vary depending on wave height, beach slope, storm surge, and sediment size (DOLAN et al., 1980), errors can be potentially large and cannot be easily quantified.

Techniques for Identifying Shorelines

The earliest historical shorelines are available from maps dating back to the late 1800's (ANDERS and BYRNES, 1991). Topographic maps are most useful for examining long-term trends in shoreline change since the maps are produced infrequently, limiting the amount of detail that can be obtained about short-term physical processes. Errors in shoreline location derived from maps may be attributed to surveyor error in identifying the shoreline feature, distortion of source maps (folding, tearing, shrinkage), and changes in the reference datum (ANDERS and BYRNES, 1991).

Since the 1920's, aerial photographs have been used to document shoreline position and change (ANDERS and BYRNES, 1991). Aerial photographs are first transformed to map coordinates using ground control points and then a proxy for the shoreline is digitized (CROWELL et al., 1991). Aerial photographs were generally collected more frequently than maps were made and, therefore, may be used to develop a more detailed understanding of short-term shoreline variability. For unrectified aerial photographs, accuracy within or between images is limited by scale differences (caused by aircraft altitude changes), by camera geometry, by ground relief (CROWELL et al., 1991; DOLAN et al., 1980; HAPKE and RICHMOND, 2000), and by the precision of the digitizing equipment and of the operator in following the trace of the HWL (ANDERS and BYRNES, 1991). Since the errors in measuring a shoreline from aerial photographs are not independent, cumulative errors may be large. CROWELL et al. (1991) estimate the total (operational) combined error for 1:10,000 scale, non-tidal coordinated, aerial photography to be ~ 7.6 m, not including errors associated with inaccurate interpretation of the location of the HWL.

Many of the errors associated with aerial photographs can be eliminated or reduced before features are identified within the image by using recent techniques involving softcopy photogrammetry where digital stereo images are used to georeference the image and remove distortion (HAPKE and RICHMOND, 2000). Elevation contours are generated on the photograph through the creation of a digital terrain model and shoreline position, or a specified contour, can be measured from the stereo pair (OVERTON and FISHER, 1996). The accuracy of the extracted features depends on the known camera parameters, flight elevation, accuracy of ground control points, and the resolution of the image (HAPKE and RICHMOND, 2000). While the use of accurate digital images eliminates much of the error associated with aerial photographs, the process of identifying a shoreline and then extracting it from an image is very labor intensive and makes the analysis of large areas more difficult.

Shorelines have also been measured from ground-based surveys of cross-shore profiles of beach elevations. Since these surveys are relatively inexpensive to perform, closely spaced profiles can be collected frequently and used for detailed studies of short-term variation in shoreline change over a limited region (MORTON, 1991). While ground-based profiling techniques may yield an accurate measure of shoreline location, the measurements are spatially limited due to the intensive labor requirement of profiling. More recently, shoreline position has been measured using vehicle-mounted, ground-based GPS (global positioning system) surveys. All-terrain vehicles equipped with GPS antennae can quickly survey shore-parallel and shore-normal profiles (MORTON et al., 1993), a single transect along the length of the beach (100 km or more in length) (LIST et al., in press), or a complete, detailed mapping of beach topography (4 km or more in length) (PLANT et al., 1996; RUGGIERO et al., 1999; RUGGIERO and VOIGT, 2000). Horizontal accuracy of shoreline positions measured using these techniques depends on, among other things, GPS accuracy, proximity of survey lines to the exact location of the shoreline, and beach slope. For example, using the vehicle-based mapping systems, on a beach with a 1:50 slope, the horizontal error in position is approximately 2.5 to 5.0 m (RUGGIERO et al., 1999).

While the spatial coverage of the vehicle-based GPS ground surveys can be very extensive, it is still somewhat limited compared to the capabilities of an airborne system. Recent developments in GPS and scanning airborne laser capabilities have made available extensive data sets of fully three-dimensional beach topography. These highly accurate and spatially dense surveys allow the possibility of making an objective and detailed determination of regional-scale shoreline position. Using laser data to quantify shoreline position and change over regional scales will contribute to an improved understanding of large-scale coastal behavior on both long-term and short-term (storm) scales.

Our objective is to develop a technique for measuring shoreline position from laser altimetry data. First, we describe the details of the lidar system and the lidar shoreline extraction technique. We then discuss the results of the ground truth test in the Outer Banks of North Carolina in September 1997. Additionally, the advantages and limitations of lidar data as a measure of large-scale shoreline position are illustrated through examination of three data sets of shoreline position collected at Assateague Island, Maryland/Virginia. Finally, we examine the statistics and longshore variability of the response of the island to the northeaster storm season of 1997–1998 using lidar-derived shorelines and beach slopes.

METHODS

Airborne Topographic Mapper

NASA's Airborne Topographic Mapper (ATM) is a scanning laser altimeter originally developed to study climate change by mapping changes in the thickness of the Greenland ice sheet (KRABILL et al., 1995). Recently the ATM has been mounted in a Twin Otter aircraft and used for mapping coastal change and assessing storm impacts on subaerial beaches (KRABILL et al., 2000; SALLENGER et al., 1999b). The ATM sur-

veys elevation with a blue-green laser reflected towards the beach using a rotating mirror that produces an elliptical scan pattern. The ATM only records the first reflection of the laser so returns are also obtained from the surface of the water.

GPS determines aircraft position and an inertial navigation system (INS) measures the aircraft's pitch, roll, and heading (KRABILL *et al.*, 1995). The process of deriving elevation measurements from the ATM system is explained in SALLENGER *et al.* (in press). Elevation data can be obtained at a rate of 50–70 km/hr (based on an aircraft speed of 110–150 knots and multi-pass coverage). In a five-hour flight mission, the ATM can completely cover 250–350 km of coast with four overlapping passes, yielding a typical combined swath width of 600–700 m. Partially overlapping passes are flown to fully cover the region of interest, to eliminate gaps in the data, and to increase data density. The footprint, and subsequent horizontal resolution, of the laser is approximately one meter in diameter and an individual laser shot is collected every 2 m^2. The ATM beach surveys provide a dense data set of subaerial beach topography with both large spatial coverage and high spatial resolution.

Extensive tests of the vertical accuracy of the ATM instrument were conducted during the SandyDuck Nearshore Processes Experiment (SandyDuck) at the U.S. Army Corps of Engineers Field Research Facility (FRF) in Duck, NC from September to October 1997. Several GPS ground-based surveys of the beach were compared to ATM surveys of the same area. The root-mean-square (rms) vertical error attributed to the ATM was 15 cm (SALLENGER *et al.*, in press). This represents a total error estimate that includes the many potential sources of error and bias for the lidar system. Based on this error estimate and a typical beach slope of 0.1, we can expect to obtain horizontal shoreline accuracy of ± 1.5 m, an order of magnitude better than typical accuracies associated with shorelines from non-stereo aerial photographs. Therefore, the lidar data may offer an alternative to the traditional techniques for measuring shorelines by easily providing objective estimates that are spatially extensive, synoptic, and of sufficient accuracy to resolve a wide range of beach variability (horizontal changes in shoreline position > 2.1 m).

Shoreline Extraction from Lidar Profiles

The technique for extracting shoreline position, x_s, from ATM data is straightforward. For any particular longshore location, y', a cross-shore profile is extracted from the irregularly spaced full data set. Data from a 2 m wide band around the profile location ($y' \pm 1$ m) are included in the individual profile. The cross-shore profiles are extracted at any constant longshore spacing, dy, ($dy = 20$ m and 10 m for this work) chosen to resolve a particular scale of longshore variability. These profiles also allow determination of other important beach parameters such as beach slope and the location and elevation of the berm, dune base, and dune crest.

After the profiles have been created, any elevation datum, z_s, or elevation-based definition of shoreline, can be extracted. Lidar data contaminated by waves and runup are first eliminated from each profile by removing all of the data points that lie seaward of the intersection of the water (identified

by the noisy laser returns, see Figure 1a) and beach. Along each lidar profile, the data are limited to a vertical range (typically $\pm$ 0.5m) around the specified elevation datum (Figure 1a). The range around the datum may be site specific and should be selected to minimize errors due to laser data in the foreshore area that still may be somewhat contaminated by returns from wave runup. A linear regression is then fit through these data with beach elevation, z_b, as the independent variable (Figure 1b). Finally, the function is evaluated at z_s to identify the horizontal position of the shoreline, x_s (Figure 1b, asterisk). The slope of the foreshore region, β, is also directly measured on each profile as the slope of the regression through the data around z_s. This procedure is repeated in the longshore for each profile to create a map of shoreline location.

Typically, there are as many as 15–20 laser shots on a profile within the range of the shoreline datum, resulting in a statistically robust regression and estimate of shoreline position. Horizontal error bars, δ_x, on x_s (Figure 1b) represent the 95% confidence interval on the mean value based on a Student's t distribution of the errors with N-2 degrees of freedom (where N is the number of points in each regression). The error bars represent the scatter present in the data and account for the random error (noise) of the system. There may also be biases, unaccounted for in these error bars, which may include, but are not limited to: bias in the range walk correction of the instrument, bias in the INS data, instrument mounting bias, or a low-frequency drift of the GPS systems (see below, as well as SALLENGER *et al.* (in press) for details).

RESULTS

Ground Truth Testing

The shoreline extraction technique was tested using laser altimetry data collected on the Outer Banks of North Carolina in September 1997 as a part of the SandyDuck experiment. The data used in the following example were collected along a 55 km stretch of coast between Corolla and Oregon Inlet (Figure 2, lower left) on September 26, 1997. Relatively straight, sandy, barrier island beaches characterize this coastline. Beach slopes, as measured from lidar data, ranged from 0.05 to 0.11, with a mean value of 0.08. The wave conditions on this day, measured by a waverider buoy in 18 m of water at the FRF in Duck, NC, were relatively calm with a deep-water wave height, H_0, of 0.57 m and a peak wave period of 7.6 s.

As a part of the SandyDuck experiment, GPS-based ground surveys were conducted, providing an opportunity to ground truth shorelines measured using lidar data. Using a GPS and inclinometer-equipped all-terrain vehicle (ATV), LIST *et al.* (in press) measured the elevation and beach slope along one longshore transect from Corolla to Oregon Inlet. From these two measurements, the location of the NOAA defined mean high water (MHW, $z_s = 0.26$ m NAVD88) line was extrapolated from the ATV elevation based on the measured beach slope. Error bars on horizontal shoreline location are derived from the elevation of the driven track and an estimated variability of the measured beach slope. Details of this tech-
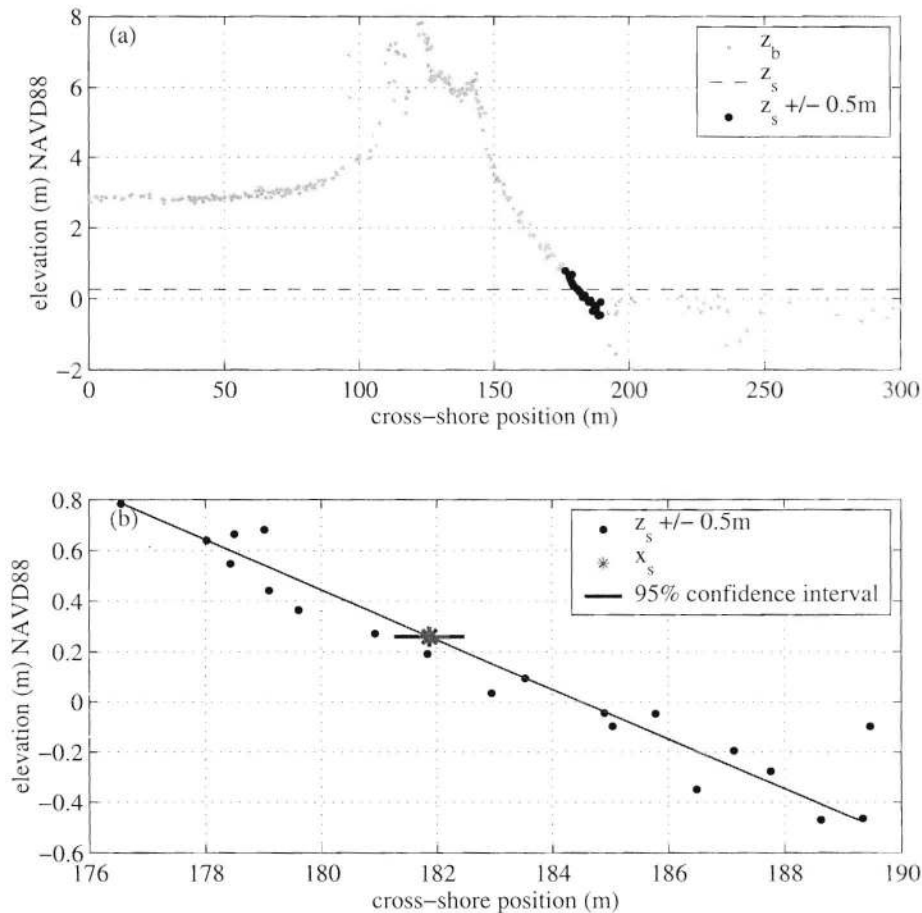
Figure 1. Lidar profile from September 26, 1997 at Kitty Hawk, North Carolina for (a) the entire cross-shore region and (b) an expanded view of the foreshore region. (a) Laser returns off of the water's surface are seen as the noisy signal seaward of $x = 190$ m. Bold symbols indicate data points (z_b) within $\pm$ 0.5 m of the MHW datum (z_s). (b) The asterisk marks the cross-shore position of the shoreline, x_s, on the foreshore. The horizontal error bar $(\pm0.42$ m) represents the 95% confidence interval about the estimate.

nique, termed the SWASH (Surveying Wide Area Shorelines) system, and the calculation of shoreline location and associated error bars can be found in LIST *et al.* (in press).

The horizontal position of the lidar (ATM) shoreline, $x_{s.atm}(y)$, was compared to the SWASH shoreline, $x_{s.swash}(y)$ to test the accuracy of the technique. The shoreline position derived from lidar profiles compares well to the SWASH shoreline with an rms difference, $(\Delta x_s)_{rms}$, of 2.9 m (Figure 3). Based on the rectangular coordinate system used, positive values of Δx_s indicate that the lidar shoreline is generally seaward of the SWASH shoreline; the mean offset, $\overline{\Delta x_s}$, between the two shorelines was 2.12 m.

The longshore distribution of shoreline position differences between the two systems, Δx_s and their combined error bars are shown in Figure 4a. In the northern part of the study region, the differences between the two techniques are not statistically significant because the 95% confidence interval for the differences lies around zero. In the southern part of the study region, where the lidar shoreline tends to fall seaward of the SWASH shoreline, there are more significant differences between the two systems. This may be partially due

to lidar data points included in the polynomial fit that are actually returns off of wave runup rather than the actual beach surface. While most of the returns from the water's surface are removed from the profile prior to shoreline extraction, a few contaminated returns sometimes remain within the range of z_s. This may serve to flatten out the regression and pull $x_{s.atm}(y')$ seaward.

Another reason for the seaward bias may be due to extrapolation errors within the SWASH data caused by the large distance between the MHW contour and the track driven the ATV on this particular day. Estimating the location of the MHW line by extrapolating along a steep slope that may tend to flatten lower in the profile will cause the location of the shoreline to fall more landward than it truly is. The beach slopes used in the SWASH system for the extrapolations were compared to foreshore slopes measured directly around the shoreline vertical datum using the lidar data. In locations where the slope used by SWASH was steeper than that measured around z_s by the ATM, the largest discrepancies between the two systems occur with SWASH estimates falling more landward of the ATM shoreline.
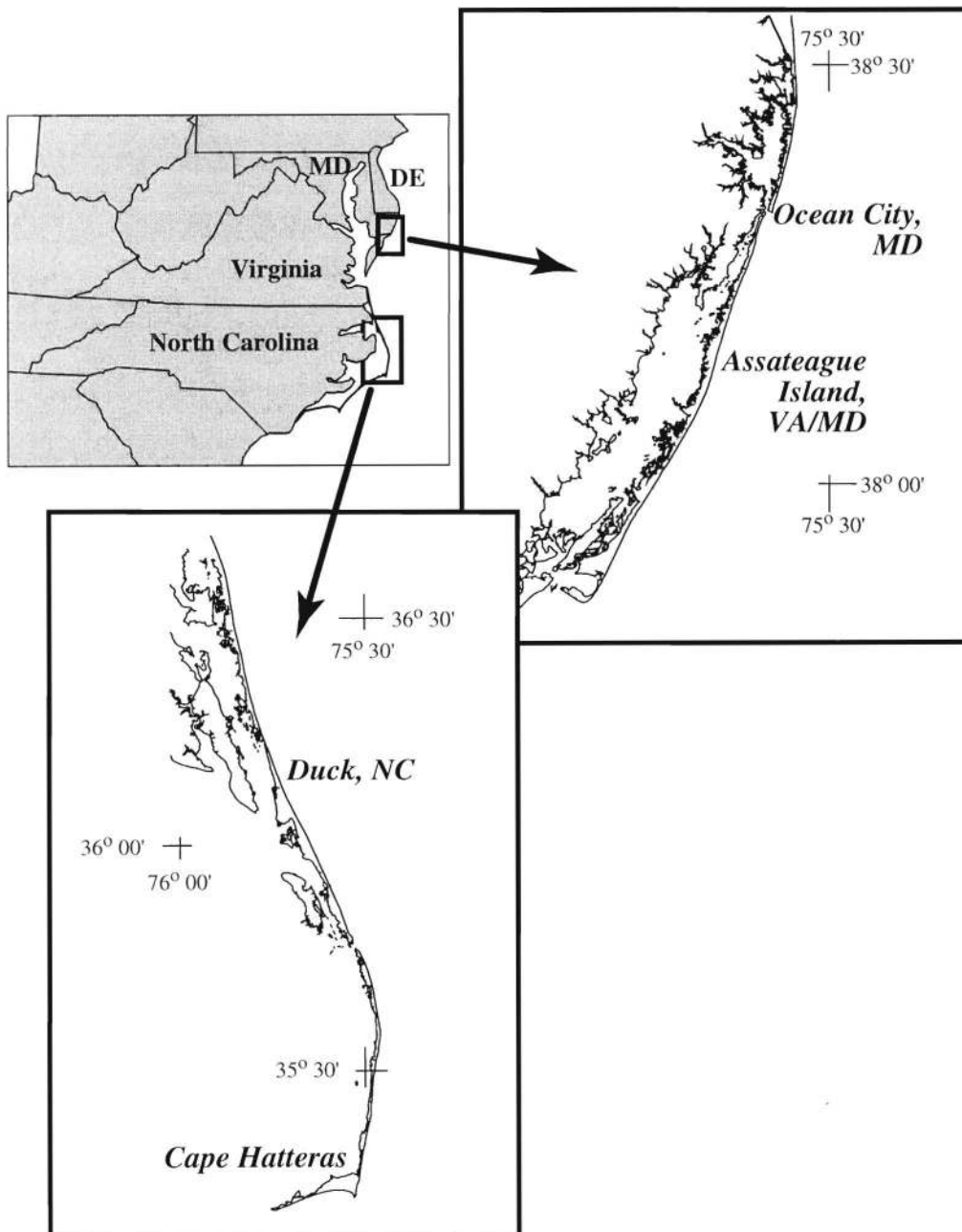
Figure 2. Location map of Duck, North Carolina (lower left) and Assateague Island, Virginia/Maryland (upper right).

Figure 4b shows the longshore structure of the individual error bars for each system. The mean horizontal error bar, $\bar{\delta}_x$, for x_{s_atm} was ± 1.4 m. These error bars represent the random noise of the system and robustness of the data used in the regression. For the lidar-derived shorelines, the largest error bars occur on profiles where only three data points were used in the regression and the R^2 value of the regression was low. This occurred in areas of low data density where there were an insufficient number of lidar data points to clearly define the foreshore. The mean error bar for x_{s_swash}, based on

assumptions of the typical variations in β, was ± 1.7 m (LIST et al., in press). For the SWASH system, error bars are calculated directly from slope and distance from the datum; hence, the error bars are larger on flatter beaches and in locations where the vehicle drove farther away from the datum.

Extensive comparisons of individual, raw ATM and SWASH data points reveal a mean vertical difference, Δz_b, between the two of 8.7 cm (SALLENGER et al., in press). This vertical difference is thought to be primarily due to a low
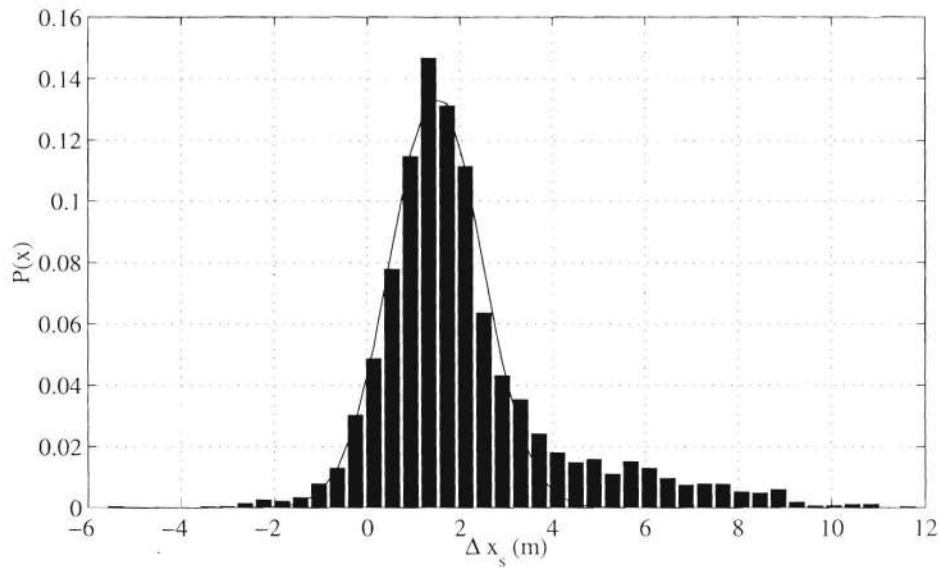
Figure 3. Probability density function of differences between ATM and SWASH estimated shoreline positions, Δx_s. The rms difference, $(\Delta x_s)_{rms}$, is 2.90 m and the mean difference, $\overline{\Delta x_s}$, is 2.12 m.
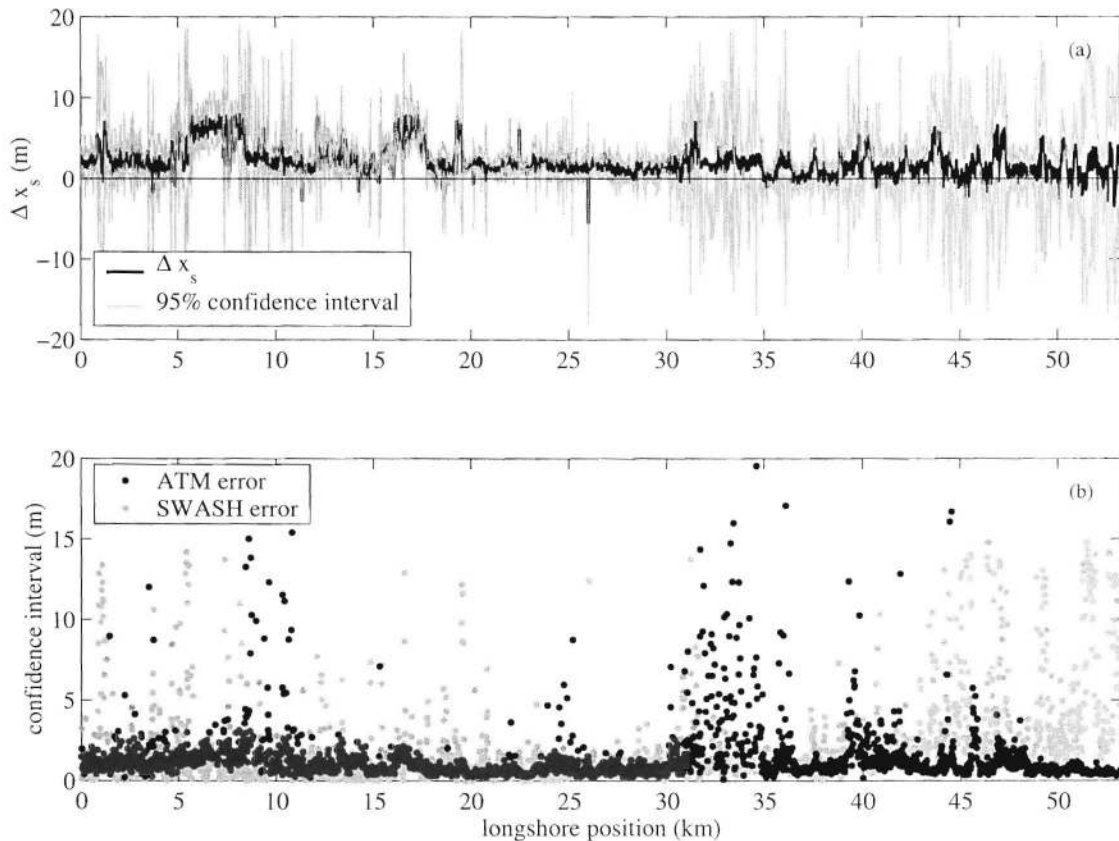

Figure 4. Longshore distribution of (a) differences between ATM and SWASH estimated shoreline positions, Δx_s, and (b) ATM and SWASH error bars for September 26, 1997 in Duck, NC. The mean horizontal error bar for x_{s_swash} was ± 1.7 m, and the mean horizontal error bar, $\overline{\delta}_s$, for x_{s_atm} was ± 1.4 m.

frequency drift inherent in both the ATM and SWASH GPS systems. This low-frequency drift is specific to GPS systems, in general, and is not particularly well understood or documented. Based on a mean GPS drift of 8.7 cm and a mean beach slope of 0.08, the site-specific, horizontal error attributable to low frequency drift is on the order of ± 1 m. (This horizontal GPS drift error is separate from the system noise error discussed above.) Since the GPS drift error has been realized just recently, the amount of drift at different sites generally will not be known. Several tests of stationary GPS systems (separate from the lidar GPS equipment) have been performed in different parts of the country and reveal a low frequency vertical drift of 6 to 8 cm over an hour period (SALLENGER *et al.*, in press). Based on this estimate, we feel the ± 1 m horizontal drift error is a conservative estimate and may be smaller in some locations. The total vertical accuracy of the ATM system (15 cm) is a bulk estimate representing all potential error sources, including this GPS drift (SALLENGER *et al.*, in press). Details of the comparisons between the raw data points and of the GPS drift can be found in SALLENGER *et al.* (in press) and KRABILL *et al.* (in press).

The vertical offset between the raw ATM and SWASH data contains a trend that decreases to the north. In the southern region of the study area $\Delta z_0 = 12$ cm while in the northern region $\Delta z_0 = 2$ cm. In order to examine the robustness of the technique and the ideal, expected error in the absence of GPS low frequency drift, the longshore trend in vertical differences due to the drift was removed from the lidar elevation data. The corrected $x_{s\_atm}(y)$ was then compared to $x_{s\_swash}(y)$ which, for our ground truth study, represents the 'real' shoreline position. The corrected lidar-derived shoreline position closely agrees with the SWASH-derived shoreline with an rms difference, $(\Delta x_s)_{rms}$, of 1.49; however it is still somewhat seaward of the SWASH shoreline; $\overline{\Delta x_s} = 0.44$ m. Reasons for this seaward bias are explained above.

Application to Shoreline Change

The technique for extracting shoreline position from lidar profiles was applied to laser altimetry data collected on Assateague Island in 1997 and 1998. Assateague Island is an undeveloped stretch of barrier island along the eastern shore of Maryland and Virginia (Figure 2, upper right). The moderately straight coastline is marked by areas of relatively high dunes alternating with low-lying areas that are frequently overwashed during large storm events. Shoreline position was measured over 60 km of coast from three lidar data sets. The first was collected on September 15, 1997 (1600–1900 GMT) before the start of the winter storm season. The second overflight was on February 9, 1998 (1600–1900 GMT), after the passage of two major northeaster storms where maximum wave heights exceeded 7 m (SALLENGER *et al.*, 1999a). Two months later on April 3, 1998 (2200–2300 GMT), a third survey was conducted that documented the initial recovery stage for the island.

The tide level and wave conditions during the February 9, 1998 ATM flight were much higher than conditions during the other two surveys (Figure 5). In order to quantitatively assess whether the MHW contour was seriously contaminated by wave runup on the February 9, 1998 profiles, the total water level (the tide level, η, plus the runup due to waves) was calculated for each survey date. The elevation of the total water level represents a maximum, not mean, total water level due to the superposition of wave crests. The 2% exceedence values for runup estimates, $R_{2\%}$, were based on an empirical formulation of HOLMAN (1986),

$$R_{2\%} = H_0(0.83\xi_0 + 0.20), \quad \text{where} \tag{1}$$

$$\xi_0 = \frac{\beta}{\sqrt{\dfrac{H_0}{L_0}}}, \tag{2}$$

ξ_0 is the Iribarren number, and L_0 is the deep-water wavelength. Foreshore beach slope, β, was measured from each lidar profile. Data on wave height and period were obtained from NDBC station 44009 located outside of Delaware Bay. Tide data were obtained from NOAA tide gauge 8570283 located near Ocean City Inlet, Maryland. Wave heights and tide levels during the February 9, 1998 survey ($H_0 = 3.0$–2.5 m) were both greater than that during the other two surveys ($H_0 \sim 0.7$ m on September 15, 1997 and $H_0 \sim 1.0$m on April 3, 1998). The total water elevation on February 9, 1998 during the lidar flight was 3.04 m, well above the elevation of MHW, 0.31 m NAVD88 (Figure 5b). Since the MHW datum was obscured in the February 9, 1998 data by elevated tide levels and large wave runup, z_s extracted for the Assateague data set was 0.81 m (0.5 m above MHW), which still lies on the active foreshore of the beach.

Shorelines were calculated from all three data sets along the 60 km stretch of beach at profiles spaced 10 m in the longshore. (The 10 m spacing was selected for a different application of the data in which smaller scale shoreline features were studied.) Figure 6 illustrates two example profiles from September 1997 and February 1998. The large scatter seaward of x = 550 m is due to the reflection of the laser off of the water's surface. Since data passes are combined, the surface appears more like noise than actual waves. Along this profile, a well-defined berm was completely eroded and the shoreline recessed 32.4 $\pm$ 0.8 m.

Shoreline change was computed for all 5730 profiles between September 1997 and February 1998 (Figure 7, black line) to examine the spatial variability of the response of the beach to the extreme storm events on January 28, 1998 and February 5, 1998. Error bars, indicating the 95% confidence interval about each estimate of shoreline change, were calculated as the rms of the combined variance of the two individual measures of shoreline position. The mean shoreline change indicates approximately 28.6 $\pm$ 0.02 m of erosion; however, there is substantial spatial variability in the data (standard deviation of shoreline change, $\sigma(\Delta x_s)$, = 16.2 m), ranging from nearly no net change to a maximum of ~150 m of erosion.

The shoreline position calculated from the April 1998 data set shows that the post-storm beach had started to recover to the pre-storm conditions (Figure 7, gray line). The mean shoreline change during this two-month recovery period was approximately 13.5 $\pm$ 0.02 m of accretion ($\sigma(\Delta x_s) = 11.0$ m). Both storm and recovery curves of shoreline change show the
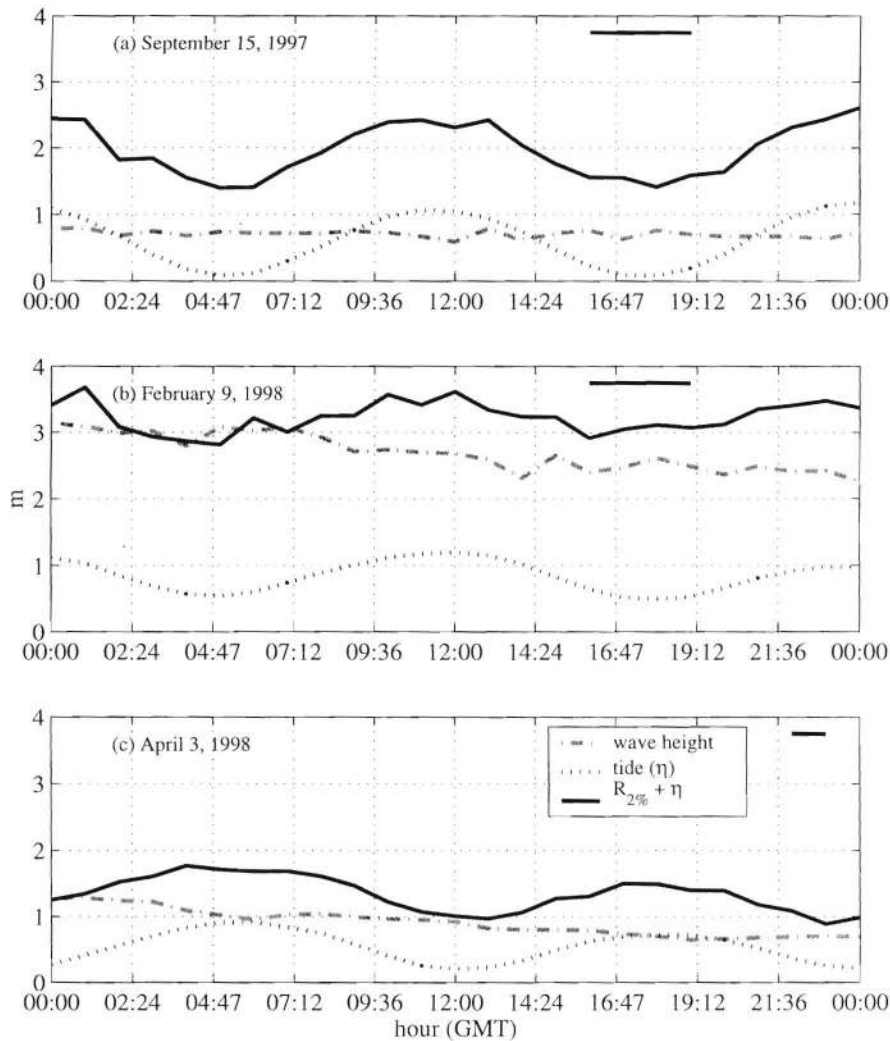
Figure 5. Wave height, tide level, and total runup during the three Assateague lidar flights on (a) September 15, 1997, (b) February 9, 1998, and (c) April 3, 1998. Total runup elevation of February 9, 1998 was much higher than during the other two flights, making the extraction of the MHW contour (z = 0.31 m) very difficult on this day. The solid horizontal bar in each panel indicates the time during which the lidar data were collected.

same order of longshore variability and the same general pattern. This is shown by a negative correlation between the two shoreline change curves with an R^2 value of 0.27, which is significant for the 95% confidence interval (N = 5170, R^2_{sig} = 0.001). This spatial pattern of erosion and accretion was not documented until recently along the Outer Banks, North Carolina and Cape Cod, Massachusetts by LIST and FARRIS (1999). The advent of the lidar system makes it possible to reveal this type of behavior over large areas and provides a means to study the longshore variability of coastal change.

Another measure of beach morphology that can be easily obtained from the laser altimetry data is beach slope, β, calculated from the regression in the shoreline extraction technique. The spatially dense data allows us to measure the spatial variation of beach slope over large areas. Figure 8 presents three probability density functions of beach slope cal-

culated along Assateague Island from lidar data. The pre-winter beach slopes (Figure 8a) are normally distributed with a mean value, $\bar{\beta}$, of 0.13 (standard deviation of β, $\sigma(\beta)$, = 0.034). After the winter's northeaster storms, the slopes were reduced significantly, $\bar{\beta}$ = 0.054 ($\sigma(\beta)$ = 0.029), as the beach responded to large wave events (Figure 8b). The April 1998 slope distribution reveals that the beach is slowly recovering as indicated by the steepening slopes, $\bar{\beta}$ = 0.08 ($\sigma(\beta)$ = 0.032), and the increasingly Gaussian distribution (Figure 8c). While these observations are not unexpected, the collection of such an extensive set of slope and shoreline data at such high accuracy is unprecedented.

DISCUSSION

There are many research and practical management applications for lidar-derived shoreline positions. As previously
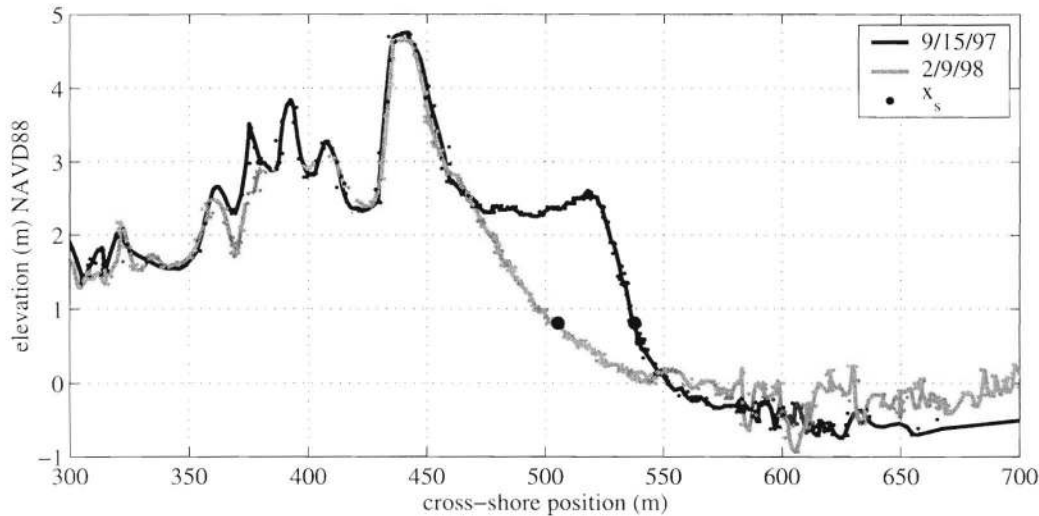
Figure 6.   Example lidar profiles for Assateague Island from September 15, 1997 (black line) and February 9, 1998 (gray line). The large solid symbol indicates the location of the 0.81 m contour (MHW + 0.5m). The 95% confidence intervals on each estimate are ± 0.28 m and ± 0.75 m, respectively. Noisy data located offshore of x = 550 m are laser returns off of the water's surface. A prominent beach berm is shown to have eroded away during the winter's northeaster storms. The mean shoreline erosion along this profile was 32.4 ± 0.8 m.

discussed, lidar shorelines can be used to study the large-scale impacts of storms on beaches. Accurate measures of large-scale, storm-induced beach change, with confidence intervals, can be determined using lidar surveys collected before and after storm events (*i.e.* Figure 7). Beach recovery can also be examined using lidar data collected some period after the passage of the storm. Profiles that are very closely spaced in the longshore will make full use of the dense three-dimensional lidar data and can be used to resolve smaller scale details of beach topography and morphologic change. Multiple lidar shorelines from one location can also be used to determine the natural variability of the shoreline position.

Studies of long-term, large-scale shoreline change are another possible use for the lidar shorelines. Accurate rates of shoreline change are of great interest today to coastal scientists, engineers, and planners. A set of profiles extracted from lidar data collected during calm weather conditions can be used to quickly and accurately determine the present location of the shoreline. The shoreline can be compared to historical shoreline positions as measured from photographs or maps to calculate rates of shoreline change.

When considering the different uses for lidar-derived shorelines, the proper selection of the vertical datum becomes important. One of the major advances of the technique discussed in this paper is that subjectivity is removed from shoreline determination since the exact location of any vertical datum for the shoreline (MHW, MHHW, *etc.*) can be easily and accurately found. The specific datum selected depends on the ultimate use of the lidar-derived shorelines. If the lidar shorelines will be compared to historical shorelines measured as wet/dry lines from aerial photographs or maps, then a vertical datum that may serve as a proxy for the digitized wet/dry line should be selected. However, such a vertical da-

tum is not clearly defined making it difficult to quantify the precise elevation of wet/dry line (see previous discussion). If lidar shorelines are to be used in conjunction with contour-based shorelines measured from ortho-rectified photographs or ground surveys, then the same shoreline datum should also be used to define a lidar shoreline. With this technique any relevant datum can be extracted from the data and used to study coastal change.

In order to obtain the most accurate estimate of the horizontal location of the shoreline datum, it is important to have dense sampling of the foreshore region. The largest error bars on shoreline location occur along profiles with sparse data due to poor lidar returns. This problem could be improved by creating wider cross-shore profiles using a larger swath region, perhaps ± 2 m.

For this technique to produce accurate estimates, it is essential that the data be collected during low tide and times of low wave energy. High tides, large waves, storm surge, and run-up may obscure the location of the vertical datum, z_s, particularly if the datum is very low on the beach face (*i.e.* MHW). If z_s lies beneath the water surface or the effect of waves and run-up, it may be necessary to look at changes occurring at a datum higher on the beach face. However, if a specific shoreline datum, such as MHW, is required, it may be possible to extrapolate to identify the cross-shore location of the shoreline, x_s, using methods similar to LIST *et al.* (in press). Future work includes expanding this technique to allow for extrapolation to the location of the shoreline datum.

We recognize that reducing the lidar data set to profiles to find shorelines is not the only way to extract the shoreline position from the data. Other research groups (*e.g.* REVELL *et al.*, in press) locate the position of the shoreline by extracting a contour from previously gridded data. While shorelines
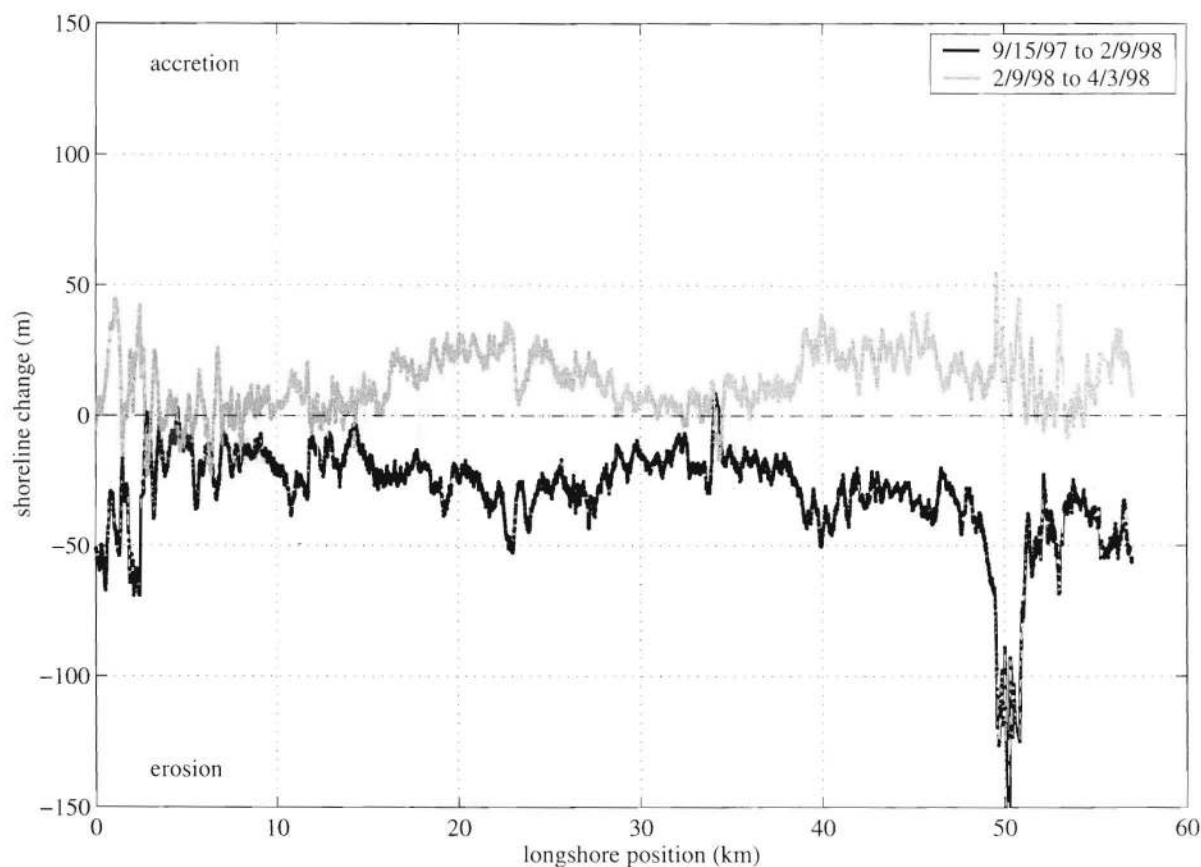
Figure 7. Shoreline change for Assateague measured from lidar-derived shorelines. Shoreline change between September 15, 1997 and February 9, 1998 (black line) shows mean erosion of 28.6 ± 0.02 m with a large amount of longshore variability. Shoreline change measured between February 9, 1998 and April 3, 1998 shows mean accretion of 13.5 ± 0.02 m with similar longshore variability. Vertical error bars indicate the 95% confidence interval about each estimate of shoreline change.

from these traditional gridding techniques are commonly used and accepted, they do not readily allow for confidence intervals to be placed on the estimates of position. This will ultimately limit the applicability of the shoreline data and subsequent measures of shoreline change. Future work will examine alternate gridding techniques, such as the quadratic loess smoother, which produce error surfaces in addition to the gridded field (SCHLAX and CHELTON, 1992). The error surface can then be used to place confidence intervals on measures of shoreline and beach volume change derived from these grids.

CONCLUSION

An objective technique has been developed for the extraction of accurate and detailed shoreline position from ATM laser data. The data from one ATM flight can provide estimates of shoreline position spaced as closely as several meters in the longshore and over large expanses (hundreds of kilometers) of coastline. While the extensive record length of historic topographic maps and aerial photographs provides a rich data set for measuring long term shoreline change, the precision and accuracy of the lidar shorelines allow for more

reliable measurement of shoreline change over shorter time periods. Lidar shorelines can be also used to establish more accurate shoreline positions for future monitoring of long-term shoreline trends.

Lidar profiles are extracted from the full three dimensional data set and a linear regression is fit to the data points within a specified range about the vertical shoreline elevation. The function is evaluated at the vertical datum to determine the cross-shore location of shoreline position. Foreshore beach slope is measured directly from the linear fit. Error bars on shoreline position represent the 95% confidence interval on each estimate based on the Student's t distribution of the errors of the regression. The accuracy of the lidar-derived shoreline was tested by comparing it to a shoreline measured using ground-based GPS techniques. The ground-based SWASH method and air-based ATM method agree closely with an rms difference of 2.9 m (1.49 m excluding a GPS drift). The longshore-averaged horizontal error bar for shorelines extracted from lidar data was ± 1.4 m for the Outer Banks and ± 1.1 m for Assateague Island.

To illustrate the power of this technique, lidar-derived shorelines were used to assess large-scale coastal change af-
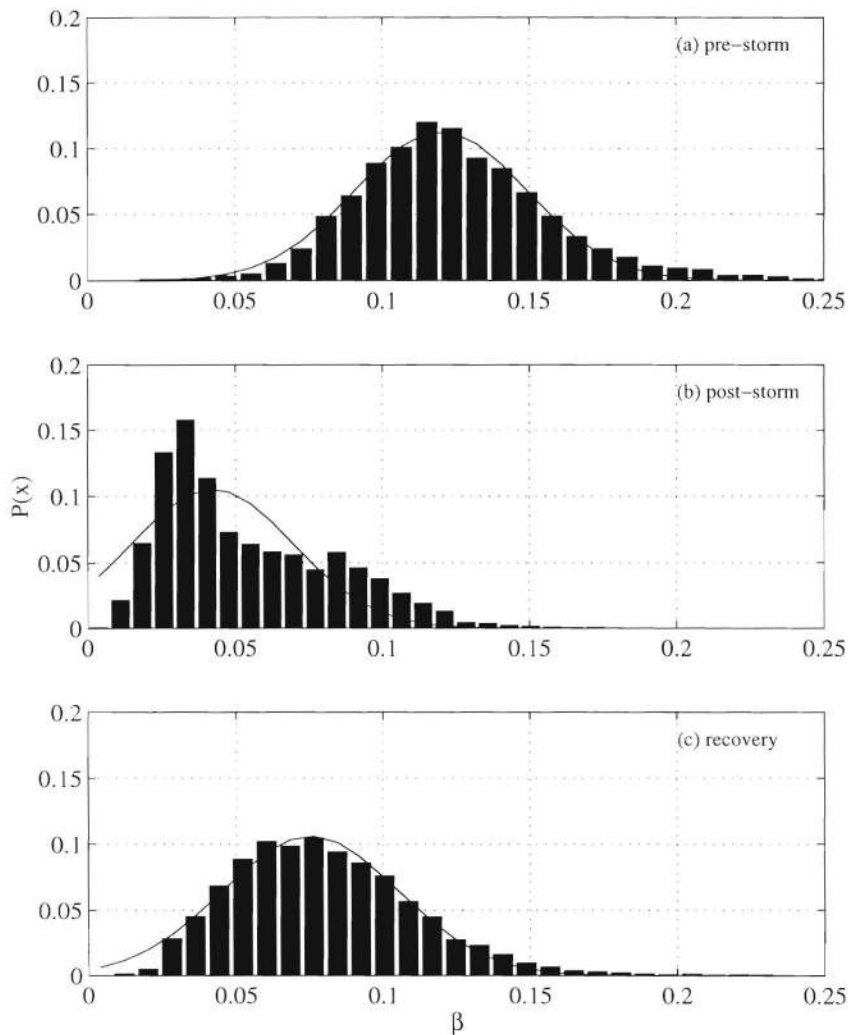
Figure 8.   Probability density functions of Assateague beach slope measured using lidar data from (a) September 15, 1997, (b) February 9, 1998, and (c) April 3, 1998. The normally distributed pre-winter beach slopes (a) are shown to significantly flatten out after the winter storms (b). The beach recovery can be seen in the increasing beach steepness measured in April (c).

ter the winter's northeaster storms along Assateague Island. After the storms, the mean shoreline change along the 60 km stretch was -28.6 ± 0.02 m with a large degree of alongshore variability, $\sigma(\Delta x_s)$, $= 16.2$ m. Shorelines measured from a survey collected after a two-month recovery period reveal 13.5 ± 0.02 m of accretion ($\sigma(\Delta x_s) = 11.0$ m). The longshore variability and distribution of beach slopes are also revealed in the lidar data. The technique showed that the mean beach slope decreased from 0.13 to 0.054 over the study area. The beach was shown to start recovering from the winter's storms as the distribution of beach slope became increasingly Gaussian and the mean value increased from 0.054 to 0.08. Using the lidar-derived shorelines, the longshore variability in the large-scale response of the coastline to storms can be accurately quantified which may lead to a more complete understanding of large-scale coastal processes.

tions to lidar data processing and profile extraction. This work was part of the USGS Coastal and Marine Program's National Assessment Project.

LITERATURE CITED

ANDERS, F.J. and BYRNES, M.R., 1991. Accuracy of shoreline change rates as determined from maps and aerial photographs. *Shore and Beach*, 59(1), 17–26.

CROWELL, M.; LEATHERMAN, S.P., and BUCKLEY, M.K., 1991. Historical shoreline change: Error analysis and mapping accuracy. *Journal of Coastal Research*, 7(3), 839–852.

DOLAN, R.; HAYDEN, B.P.; MAY, P., and MAY, S., 1980. The reliability of shoreline change measurements from aerial photographs. *Shore and Beach*, 48(4), 22–29.

HAPKE, C. and RICHMOND, B., 2000. Monitoring beach morphology changes using small-format aerial photography and digital softcopy photogrammetry. *Environmental Geosciences*, 7(1), 32–37.

HOLMAN, R.A., 1986. Extreme value statistics for wave run-up on a natural beach. *Coastal Engineering*, 9, 527–544.

KRABILL, W.; WRIGHT, C.; SWIFT, R.; FREDERICK, E.; MANIZADE, S.; YUNGEL, J.; MARTIN, C.; SONNTAG, J.; DUFFY, M.; HULSLANDER, W., and BROCK, J., 2000. Airborne laser mapping of Assateague National Seashore Beach. *Photogrammetric Engineering & Remote Sensing*, 66(1), 65–71.

KRABILL, W.B.; MARTIN, C.F.; THOMAS, R.H.; ABDALATI, W.; SONNTAG, J.G.; SWIFT, R.N.; FREDERICK, E.B.; MANIZADE, S.S., and YUNGEL, J.G., in press. Aircraft laser altimetry measurement of elevation changes of the Greenland ice sheet: technique and accuracy assessment. *Journal of Geodynamics*.

KRABILL, W.B.; THOMAS, R.H.; MARTIN, C.F.; SWIFT, R., and FREDERICK, E.B., 1995. Accuracy of airborne laser altimetry over the Greenland ice sheet. *Int. Journal of Remote Sensing*, 16, 1211–1222.

LIST, J. and FARRIS, A., 1999. Large-scale shoreline response to storms and fair weather. *Coastal Sediments '99* (Long Island, New York, ASCE), pp. 1324–1338.

LIST, J.H.; FARRIS, A.S.; IRWIN., B.; KONICKI, K.M.; HANSEN., M.E., and REISS, T.E., in press. *A vehicle -based method for quantifying shoreline position on tidal coasts as the horizontal position of the mean high water contour: methods and error assessments.* U.S. Geological Survey, Open File Report 2000.

MORTON, R.A., 1991. Accurate shoreline mapping: Past, present, and future. *Coastal Sediments '91* (Seattle, Washington, ASCE), pp. 997–1010.

MORTON, R.A.; LEACH, M.P.; PAINE, J.G., and CARDOZA, M.A., 1993. Monitoring beach changes using GPS surveying techniques. *Journal of Coastal Research*, 9(3), 702–720.

OVERTON, M.F. and FISHER, J.S., 1996. Shoreline analysis using digital photogrammetry. *25th International Conference on Coastal Engineering* (Orlando, Florida, ASCE), pp. 3750–3761.

PLANT, N.G.; HOLMAN, R.A., and BIRKEMEIER, W.A., 1996. Kinematics of alongshore propagating sand waves at Duck. *Trans. American Geophysics Union*, 77(46), 388.

REVELL, D.; KOMAR, P., and SALLENGER, A., in press. An application of LIDAR to analyses of El Nino erosion in the Netarts littoral cell, Oregon. *Journal of Coastal Research*.

RUGGIERO, P.; COTE, J.; KAMINSKY, G., and GELFENBAUM, G., 1999. Scales of variability along the Columbia River littoral cell. *Coastal Sediments '99* (Long Island, New York, ASCE), pp. 1692–1707.

RUGGIERO, P. and VOIGT, B., 2000. *Beach Monitoring in the Columbia River littoral cell, 1997–2000.* Olympia, Washington, Coastal Monitoring & Analysis Program, Washington Department of Ecology, 00–06–26.

SALLENGER, A.H.; HOWD, P.; BROCK, J.; KRABILL, W.B.; SWIFT, R.N.; MANIZADE, S., and DUFFY, M., 1999a. Scaling winter storm impacts to Assateague Island, MD, VA. *Coastal Sediments '99* (Long Island, New York, ASCE), pp. 1814–1825.

SALLENGER, A.H.; KRABILL, W.; BROCK, J.; SWIFT, R.; JANSEN, M.; MANIZADE, S.; RICHMOND, B.; HAMPTON, M., and ESLINGER, D., 1999b. Airborne laser study quantifies El Nino-induced coastal change. *EOS, Transaction American Geophysical Union*, 80(8), 89, 92–93.

SALLENGER, A.H.; KRABILL, W.; SWIFT, R.; BROCK, J.; LIST, J.; HANSEN, M.; HOLMAN, R.A.; MANIZADE, S.; SONNTAG, J.; MEREDITH, A.; MORGAN, K.; YUNKEL, J.K.; FREDERICK, E., and STOCKDON, H., in press. Evaluation of airborne scanning lidar for coastal change applications. *submitted to Journal of Coastal Research.*

SCHLAX, M.G. and CHELTON, D.B., 1992. Frequency domain diagnostics for linear smoothers. *Journal of the American Statistical Association*, 87(420), 1070–1081.

STAFFORD, D.B., 1971. *An Aerial Photographic Technique for Beach Erosion Surveys in North Carolina.* U.S. Army Corps of Engineers, Coastal Engineering Research Center, Technical Memorandum 36.

THORNTON, E.B.; DALRYMPLE, R.A.; DRAKE, T.; GALLAGHER, E.; GUZA, R.T.; HAY, A.; HOLMAN, R.A.; KAIHATU, J.; LIPPMANN, T.C., and OZKAN-HALLER, T., 2000. *State of Nearshore Processes Research: II.* Monterey, CA, Naval Postgraduate School, Technical Report NPS-OC-00-001.